Correlation of Autophagy-Related Genes in High Risk and Low Risk Signatures Based on Prognostic Index Model SKCM Patient

Kun Zhang
Shantou University Medical College https://orcid.org/0000-0001-5463-6512
Yan Liang
Shantou University Medical College
Ruoxi Tian
Tianjin Medical University
Ning Zeng
Guilin Medical University Affiliated Hospital
Guiying Wang
Hebei Medical University Third Affiliated Hospital
Shijie Tang (shijietang0773@163.com)
Shantou University Medical College

Research

Keywords: autophagy, skin cutaneous melanoma, prognostic, biomarker, tumor immunotherapy

Posted Date: September 15th, 2021

DOI: https://doi.org/10.21203/rs.3.rs-847313/v1

Abstract

Autophagy plays a dual role in tumor development and autophagy-related genes (ARGs) involved in the development of cancer. However, the correlation between these high and low risk ARGs is still unclear. To systematically study the relationship between ARGs and melanoma patients, the expression profiles of ARGs were integratedly analyzed based on the TCGA and GTEx dataset. The results suggested 8-ARGs marker can predict the prognosis of skin cutaneous melanoma (SKCM), 5-ARGs (*CFLAR*, *DAPK2*, *ITGA6*, *DNAJB9* and *RGS19*) were low risk index, 3-ARGs (*EIF2AK2*, *EGFR* and *PTK6*) were high risk index. Further validation showed *CFLAR*, *DNAJB9* and *PTK6* were significant related to SKCM. In tumor immunization, *CFLAR* and *DNAJB9* have stronger correlation with tumor immune cells, and there is a significant positive correlation among the low risk genes. However, there is no significant correlation between the high and low risk factors. In addition, our results also showed that *CFLAR* and *PTK6* were significantly negatively correlated with tumor purity; *PTK6* was significantly positively correlated with patient's age, *CFLAR* was significantly negatively correlated with patient's age; *CFLAR* and *DNAJB9* were significantly positively correlated in purity and age. It provides a new prognostic indicator for patients and a new idea for the mechanism of autophagy in melanoma.

Introduction

As one of most aggressive type of cancers worldwide, Skin cutaneous melanoma (SKCM) is originated from melanocytes [1–5]. SKCM shows clear differences in incidence, mortality, genomic profile, and anatomic presentation, depending on the country of residence, ethnicity, and socioeconomic status [6]. Cutaneous melanoma accounts for approximately only 5% of all skin malignancies, but is thought to be the most invasive and lethal form [6]. Once malignant melanoma metastasis occurs, it develops faster than all other solid tumors [7]. Despite recent advances in curative surgery and adjuvant therapy, the mortality is still high due to its late detection and high recurrence rates [8]. Therefore, there is an urgent need to find new molecular markers to predict the prognosis of SKCM patients.

Autophagy is a multi-step lysosomal degradation process, which is initiated from the formation of autophagosome to deliver the protein and cell organelle to lysosome for degradation. This catabolic process is involved in a variety of autophagy-related genes (ARGs), which has been extensively studied and been proven involved in the development of cancer [9–13]. However, autophagy is suggested to have both tumor-suppressing and tumor-promoting functions during cancer progression, depending on the type and stage of tumor [14]. The role of autophagy in tumorigenesis is still controversial, and its mechanism is still imperfect and uncertain. Autophagy has a complex function in the development of tumor. It is an urgent problem to further explore the potential biological process of autophagy in tumorigenesis and development [15].

A large number of studies have shown that autophagy is also essential for maintaining cellular homeostasis in the skin and reported a correlation between autophagy and SKCM [16–19]. For example, CX-F9 inhibits the malignant phenotype of melanoma cells and down-regulation of ATG5 contributes to

tumorigenesis in early-stage cutaneous melanoma [18, 20]. Modulation of autophagy contribute to the regulation of melanocyte biology and skin pigmentation [17]. Recently research showed 7-DEARG signature could be regarded as an independent prognostic signature in clinical setting, and nomogram may supply a more simple and accurate prediction for the prognosis of melanoma [21]. However, there is rarely study revealed correlation between these prognostic signature ARGs. The purpose of this study was to gain insight into the potential clinical utility of ARGs for prognostic stratification and to investigate the correlation and characteristics of ARGs.

According to the tumor lymph node metastasis (TNM) classification system, pathological staging is commonly used to predict the survival rate of patients [22, 23]. Other factors, such as age, performance status, and tumor location, also affect patient survival [24, 25]. In recent years, nomograms have gradually gained popularity, which use different clinical variables to determine a statistical prognostic model that generates a probability of clinical outcomes for an individual patient [15, 26]. Nomograms have been applied in various types of cancers to establish a prognostic nomogram, which can help in prediction of early bone metastases for patients with breast cancer [27]. Therefore, our research obtained prognostic ARGs index by combining TNM and nomograms system model, and explored the correlation signature through GEPIA and TIMER database, which facilitate the development of personalized prognostic information for SKCM patients.

Result

Identification of prognostic ARGs in melanoma

RNA-seq and clinical data from 472 SKCM tissue samples and 1 non-tumor samples were downloaded from TCGA. Only 210 ARGs showed expression values in TCGA database. Finally obtained 49 up-regulated and 45 down-regulated ARGs according to FDR<0.05 and [log2(fold change)]>1 (Figure S1A and 1B) and a scatter plot was visualized to show the expression pattern of 94 differentially expressed ARGs between melanoma and non-tumor tissue (Figure S1C). In addition, functional enrichment analysis of 94 differentially expressed ARGs provides a biological understanding of these genes. GO enrichment shows that the biological process of differential genes is mainly involved in autophagy and process utilizing autophagic mechanism, the molecular functions is mainly involved in ubiquitin protein ligase binding (Figure S1D). KEGG enrichment shows that pathways of differential genes mainly involved pathways in autophagy, apoptosis, shigellosis and human papillomavirus infection.

To analyze ARGs involved in skin cutaneous melanoma progression, ARGs were significantly associated with prognosis. The forest map of the hazard ratio indicates that most of these genes are protective factors, 14 high risk genes (*ULK*, *SPNS1*, *TP63*, *HSP90AB1*, *BAK1*, *GAPDH*, *ATG9B*, *EEF2K*, *BNIP3*, *PTK6*, *BIRC5*, *DAPK1*, *PARP1* and *EGFR*) and 22 low risk gens (*PRKCQ*, *CASP3*, *CALCOCO2*, *DAPK2*, *ATG16L2*, *EDEM1*, *SERPINA1*, *FAS*, *KIF5B*, *VAMP7*, *APOL1*, *CCR2*, *ITGA6*, *DNAJB9*, *GAA*, *CFLAR* and *CXCR4*) (Figure 1A). Both GO (GO:0006914) and KEGG (hsa04140) analysis showed that these genes are closely related to autophagy process (Figure 1B and 1C). 57% high risk genes were down-regulated in melanoma, 72%

low risk genes were up-regulated in melanoma. Given the important clinical implication of these ARGs, we examined that mRNA genetic alterations of these genes and found that amplification is the most common type of mutations (Figure 1D). A total of 13 genes have a mutation rate ≥ 5%, of which *TP63* is the most frequently mutated gene (17%).

Establishment of Autophagy-Related Signature in Training Set and Validation Set

Patients in TCGA dataset was randomly assigned in a 5:5 ratio to training set and validation set with the same proportion of each SKCM stage. 36 differentially expressed ARGs were initially subjected to univaritate Cox proportional hazards regression analysis in the training set and validation set. We constructed autophagy prognostic index (API) to divide SKCM patients into two groups (high-risk and low-risk) with discrete clinical outcomes for overall survival (OS). The result showed 8 ARGs were significantly associated with the OS (P<0.05). These include 2 risky genes and 6 potential protective genes. Figure 2 showed autophagy-related signature in training set and validation set. Distribution of prognostic index in TCGA dataset was showed in Figure 2A, survival status of patients in different groups was showed in Figure 2B and heatmap of the expression profile of the included ARGs was showed in Figure 2C. To determine the performance of the API in predicting clinical outcomes in skin cutaneous melanoma patients, Kaplan-Meier survival curves were plotted to analyze different survival times between high-ris and low-risk groups. Kaplan-Meier analysis showed that patients with high-risk group was significantly lower than that in the low-risk group (Figure 2D).

Univariate analysis (HR=1.186, 95%, CI=1.121-1.254, P<0.001) showed that ARI was significantly associated with patient prognosis (Figure S2A). In addition, after adjusting for clinicopathological features such as age, tumor subtype, tumor size, and lymph node metastasis, API remined an independent prognostic indicator for SKCM patients in multivariate analysis (HR=1.194, 95%, CI=1.129-1.263, P<0.01) (Figure S2B). In the validation set, the distribution of survival status and risk scores of patients have a similar trend to that in the training set. Consistent with the results in the training set, survival analysis showed a significantly lower OS (P<0.001). The overall analysis showed the area under the curve of the corresponding receiver operating characteristic (ROC) curve for 1 year, 3 years, and 5 years of survival is 0.725, 0.696 and 0.740, respectively. The training set showed the ROC for 1 year, 3 years and 5 years of survival is 0.732, 0.810 and 0.854. The test set showed the ROC for 1 year, 3 years and 5 years of survival is 0.720, 0.583 and 0.634. This indicated that the prognostic index based on ARGs has a certain potential in survival prediction (Figure S2C.

Validation of significant autophagy-related genes index for SKCM patients

To Construct validation of nomogram, we subsequently analyzed the relationship between ARGs prognostic index and clinical features. Significant increase in risk score were in metastasis (Figure S3A), late clinical stage (Figure S3B), in larger tumor size (Figure S3C). A weighted total score calculated from each variable was used to estimate the 3- and 5- year OS of patient with SKCM (Figure S3D). The result showed gender, age, stage and risk score were significant risk factors for patients with SKCM (*P*<0.05).

The calibration plots showed well correlation between observed OS and nomogram predicted OS (Figure S3Eand S3F).

The survival curve of single gene showed that high expression of *CFLAR*, *DAPK2*, *EIF2AK2*, *ITGA6*, *DNAJB9* and *RGS19* were significantly related to the increasing survival rate of patients, and low expression of *EGFR* and *PTK6* were closely related to clinical prognosis (Figure 3A). Overall survival analysis of GEPIA showed expression level of *RGS19*, *EIF2AK2* and *EGFR* had not related to patient survival (Figure 3B). Besides, stage profile suggested that only *CFLAR*, *DNAJB9* and *PTK6* had clinical stage relevance (Figure 3C).

Relationship between the expression of targeted ARGs and immunity in SKCM

To reveal the relationship between the expression level of significant ARGs in melanoma and immunity, we downloaded the score data of six kinds of immune infiltrating cells of SKCM from timer, and respectively analyzed the correlation between the expression of *CFLAR*, *DNAJB9* and *PTK6* and the proportion of these cells. Our results showed that *CFLAR* was positively correlated with the scores of six kinds of immune. Among them, cells_ Neutrophil had the highest correlation with *CFLAR* and B_Cell correlation was the lowest. *DNAJB9* showed significant positive correlation with B_cell, CD8_Tcell, Timer-Neutrophil, Timer_Marcrophage and Dendritic. The correlation of *DNAJB9* with Timer_neutrophil was the highest. *PTK6* only significantly negative correlated to B_ Cell (Figure 4A). In addition, the results showed that only *CFLAR* was significantly positively correlated with the overall microenvironment score, *CFLAR* and *DNAJB9* were significantly positively correlated with immune score, *CFLAR*, *DNAJB9* and *PTK6* were significantly correlated with stromal score, among which *CFLAR* and *DNAJB9* were positively correlated and *PTK6* was negatively correlated (Figure 4B). Finally, considering the importance of neoantigen for personalized treatment of cancer patients, we further analyzed the correlation between *CFLAR*, *DNAJB9*, *PTK6* and neoantigen, but unfortunately, none of the three genes had significant correlation (Figure 4C). SCNA module of target genes were analyzed by TIMER, which provides the comparison of tumor infiltration levels among tumors with different somatic copy number alterations for a given gene. The results showed that the copy number of arm-level deletion of *CFLAR* was related to the infiltration of B cell, CD4+T cell, macrophage, and dendritic cell, and the copy number of arm level gain was related to the infiltration of CD4 + T cell. The copy number of *DNAJB9* arm level deletion was correlated with B cell, CD4+T cell and dendritic cell infiltration. Copy number of *PTK6* high amplification was significantly correlated with six kind immune cell lines, copy number of arm level gain was correlated with B cell, CD4+T cell, macrophage, and dendritic cell infiltration, copy number of arm level deletion was correlated with B cell, CD8+T cell, CD4+T cell, and dendritic cell infiltration (Figure S4A). Immune checkpoint genes also play an important role in tumor immunotherapy. Our result found that *PTK6* only had a significant correlation with *VTCN1*, *CFLAR* was significantly correlated with most immune checkpoint genes, but not with *TNFRSF14*, *CD276*, *VTCN1*, *HHLA2*, *CD70*, *TNFSF9*, *CD44*. *DNAJB9* significantly correlated with *CD200*, *NRP1*, *TNFSF4*, *CD28*, *CD200R1*, *HAVCR2*, *CD80*, *CD160*, *TNFSF14*, *VSIR*, *CD86* and *TNFRSF9*. There was a similar correlation between *DNAJB9* and *CFLAR*. While the correlation genes of high-risk

signature *PTK6* had almost opposite correlation characteristics with low-risk signature *DNAJB9* and *CFLAR* (Figure S4B).

Correlation between *CFLAR*, *DNAJB9* and *PTK6* in patients with SKCM

Firstly, we studied the correlation between high risk signature and low risk signature in tumor, skin-sun exposed, skin-not sun exposed groups by GEPIA. The result showed high risk signature only negatively correlated with low risk signature in the skin-sun exposed group (Figure S5A). Then we analyze the correlation between *CFLAR*, *DNAJB9* and *PTK6* by TIMER. The results showed that in the early stage of SKCM, *DNAJB9* was negatively correlated with *PTK6* and positively correlated with *CFLAR*, in the late stage of SKCM, *DNAJB9* was significantly positively correlated with *CFLAR*, in SKCM, *DNAJB9* was significantly positively correlated with *CFLAR* (Figure S5B). In addition, our results also showed that *CFLAR* and *PTK6* were significantly negatively correlated with tumor purity, *PTK6* was significantly positively correlated with patient's age, *CFLAR* was significantly negatively correlated with patient's age, *CFLAR* and *DNAJB9* were significantly positively correlated in purity and age (Figure 5).

Tissue profile and cell localization of *CFLAR*, *DNAJB9* and *PTK6*

HPA database mRNA level tissue expression level showed that *DNAJB9* was widely and highly expressed in all kinds of tissues, but especially low expression in skin. *CFLAR* was expressed in all kinds of tissues, and *PTK6* was highly expressed in stomach, small intestine, colon, duodenum, esophagus and skin, with the highest expression in skin (Figure 6A). In addition, *CFLAR* and *DNAJB9* were localized in the cytoplasm of A-431 cell line, and *PTK6* located in the nucleus (Figure 6B). The protein level of medium was detected in skin and epithelial cells (Figure 6C). In melanoma and skin cancer, *PTK6* was mainly expressed in cytoplasm and cell membrane, *CFLAR* and *DNAJB9* expressed in cytoplasm, cell membrane and nucleus.

Discussion

Autophagy plays a significant role in tumor promotion and suppression, depending on the cell/tissue types and the tumor stages, which hinders the clinical application of autophagy activators or inhibitors. Previous research have demonstrated that autophagy in involved in the regulation of melanocyte biology and skin pigmentation[17], ARGs have been reported to predict the survival of SKCM [21]. However, correlation between high risk signature and low signature is still unclear. Therefore, we aimed to identify ARGs associated with OS of patients with SKCM and explore tumor immunization and correlation of significant ARGs, thereby helping to develop individualized treatment option based on patient risk.

In present study, we identified 36 ARGs, which were dysregulated in patients with SKCM. After univariate and multivariate analysis, 8 ARGs were used to construct risk score signature using their expression levels weighted by corresponding correlation coefficient. The autophagy-related signature could divide patients into high-risk and low-risk groups based on the median risk score. Patients with high-risk score

have significantly worse OS than patients in low-risk group. Furthermore, the predictive accuracy of autophagy-related signature.

In addition, we established an autophagy-based signature s based on multi–data sets, which showed favorable predictive ability. The results of the TCGA training data set (mainly composed of the US and European populations) are well validated in the validation set of the Asian population composition. Validation in multiple countries enhances the reliability of the results, indicating that ATG scores may be appropriate for patients of different ethnicities. Moreover, our nomogram combining risk score with conventional clinical parameters shown significantly improved performance. For example, the nomogram showed a higher predictive ability than the AJCC TNM staging system, consistent with previous studies. Nomogram is of great significance to clinicians and patients because that it can predict individual patient outcomes. The proposed autophagy-related signature included 8 ARGs. All genes in the signature were associated with OS of patients with SKCM.

In this present study, *CFLAR*, *DNAJB9* and *PTK6* were further confirmed to be the significant signature for prognostic factors in melanoma, *CFLAR* and *DNAJB9* were low risk index, *PTK6* was high index, which is consistent with previous molecular experiment. It reported that overexpression of PTK6 predicts poor prognosis in bladder cancer patients [30]. And *PTK6/BRK* is expressed in the normal mammary gland and activated at the plasma membrane in breast tumors [31]. Another research illustrated the clinical potential for PTK6 inhibition to improve treatment of patients with high-risk TNBC [32]. These studies support the results of PTK6, a significant high-risk marker identified in this study based on ARGs prognostic models. The CaMKII-mediated pathway for *CFLAR (c-FLIP)* upregulation protects melanoma cells from TRAIL-induced apoptosis[33]. c-FLIP is a critical anti-cell death protein often overexpressed in tumors and hematological malignancies and its increased expression is often associated with a poor prognosis [34]. *CFLAR (c-FLIP)* also played important role on melanomas [35, 36]. *c-FLIP* might play an important role in the obtaining of aggressive biological behaviour and be useful in predicting prognosis [35]. *DNAJB9* inhibits p53-dependent oncogene-induced senescence (OIS) and induces neoplastic transformation under oncogenic RAS activation in mouse primary fibroblasts [37]. These studies support the low risk of CFLAR and DNAJB9 for prognostic factors in melanoma.

In tumor immunization, high and low risk factors seem to show opposite correlation characteristics. There is a significant positive correlation among the low risk genes, but there is no significant correlation between the high and low risk factors. *CFLAR* and *DNAJB9* have stronger correlation with tumor immune cells. In addition, our results also showed that *CFLAR* and *PTK6* were significantly negatively correlated with tumor purity; *PTK6* was significantly positively correlated with patient's age, *CFLAR* was significantly negatively correlated with patient's age; *CFLAR* and *DNAJB9* were significantly positively correlated in purity and age.

The results of tissue expression profile showed that *PTK6* was highly expressed in skin, while *DNAJB9* and *CFLAR* were low expression in skin, which may determine that *DNAJB9* and *CFLAR* are low risk index in prognostic model, and *PTK6* is high risk index. The results of localization analysis showed that

DNAJB9 and *CFLAR* had similar localization characteristics, both located in the cytoplasm and *PTK6* located in the nucleus. Whether this is related to the high and low risk needs further experimental verification. In addition, the localization of *PTK6* changed significantly in tumor patients, with nuclear transformation into cytoplasm and cell membrane[31, 38]. In normal or non-tumorigenic tissues, PTK6 promotes cellular differentiation and apoptosis.

Conclusion

In conclusion, this study conducted a novel 8 autophagy-related signature to predict OS of patients with SKCM, and studied the correlation between validated ARGs based on a comprehensive analysis of ARGs expression profiles and corresponding, which may help in clinical decision-making for individualized therapy, and identified 3 ARGs significant to SKCM prognostic. Our findings indicated that in tumor immunization analysis, high and low risk factors seem to show opposite correlation characteristics. There is a significant positive correlation between the low risk signature genes, but there is no significant correlation between the high and low risk genes.

Material And Methods

Data collection

The gene expression and clinical information of 472 patients were obtained from TCGA (https://cancergenome.nih.gov/) and 81 paracancerous tissues were obtained from GETx (https://commonfund.nih.gov/GTEx/). Use this data in accordance with TCGA and GETx relevant policies to get the gene expression, GENCODE (https://www.gencodegenes.org) Version 28 annotated probes was used to obtain the corresponding gene names. All data were obtained from TCGA and CGGA, approval for our study by the ethics committee was not necessary.

Screening of Differential Genes

The limma package of R was used to analyze glioma and corresponding normal samples, and differentially expressed mRNA were screened out. Screening criteria was based on $P<0.05$ and Fold Change>1.

Identification of prognosis-related genes

By using R/Bioconductor's "survival" package, one-to-one univariate survival analysis was performed for the differential gene expression, and the gene expression amount with P value less than 0.05 was selected for further construction of the model.

Selection of best genes for modeling.

The prognostic risk score model was established with the following formula: risk score = expression level of Gene1 × β1 + expression level of Gene2 × β2 +…+ expression level of Genen × βn, βis a regression

coefficient model calculated by multivariate Cox regression. Subsequently, a prognostic risk score was generated for each patient. All patients were divided into high risk (high risk score) and low risk (low risk score) groups according to the median of their risk score. Then, K-M survival curves were constructed to estimate the prognosis of patients with high or low risk scores, and survival differences between high and low risk groups were assessed by two-sided log-rank test. and the grouping boundary value was calculated by the "survival" package and "survminer" package of R/Bioconductor, and the resulting two groups were separately Kaplan-Meier curves were plotted. At the same time, in order to verify the validity and repeatability of the model, patients were randomly divided into training group and validation group at a ratio of 5:5 using R. In the training group, patients were divided into high-risk group and low-risk group according to the risk score. The grouping boundary value was calculated from the "survival" package and "survminer" package of R/Bioconductor, and Kaplan-Meier curves were drawn for the two groups.

Development of the gene prognostic nomogram

Using 472 training samples from TCGA, we generated a prognostic nomogram using the R package "rms" based on the expression level of genes selected in the previous step. In the software package, the "cph" function is used to construct the COX model. Based on this model, a prognostic nomogram was generated using the "nomogram" function. Line length corresponding to each variable in the prognostic nomogram reflects the contribution of predictive factors to patient prognosis.

Functional analysis

The Bohao Online Enrichment Tool (http://enrich.shbio.com/) was used to perform functional enrichment of differentially expressed ARGs. Gene Ontology (GO) and Kyoto Encyclopedia of Genes and Genomes (KEGG) were used to assess relevant functional categories. GO and KEGG enrichment pathways with P and Q values less than 0.05 are considered important categories.

Tumor immunization analysis

TIMER was applied to download score data of six kinds of immune infiltrating cells. we used R software package estimate to analyze the immune score and stromal score of SKCM samples to explore the relationship between *CFLAR*, *DNAJB9*, *PTK6* and tumor development in tumor microenvironment[28].

Correlation analysis

TIMER (https://cistrome.shinyapps.io/timer/) and GEPIA (http://gepia2.cancer-pku.cn/#correlation) were used to construct the co-expression trend correlation of hub genes in patients with SKCM-metastasis[28, 29].

Declarations

Ethics approval and consent to participate

Not applicable

Consent for publication

Not applicable

Competing interests

The authors declare no conflicts of interest.

Funding

There is no fund support for this topic.

Authors' contributions

All authors made substantial contributions to conception and design, acquisition of data, or analysis and interpretation of data, took part in drafting the article or revising it critically for important intellectual content, gave final approval of the version to be published, and agree to be accountable for all aspects of the work.

Acknowledgments

We also gratefully thank American Journal Experts for editing this manuscript.

Availability of data and materials

All data of the manuscript comes from TCGA(https://cancergenome.nih.gov/), GENCODE(https://www.gencodegenes.org),TIMER(https://cistrome.shinyapps.io/timer/) and GEPIA(http://gepia2.cancer-pku.cn/#correlation).

References

1. Holmes, D., *The cancer that rises with the sun.* Nature, 2014. **515**(7527): p. S110-1.
2. Wang, J.L., et al., *Risk of non-melanoma skin cancer for rheumatoid arthritis patients receiving TNF antagonist: a systematic review and meta-analysis.* Clin Rheumatol, 2020. **39**(3): p. 769-778.
3. Salvati, L., M. Mandala, and D. Massi, *Melanoma brain metastases: review of histopathological features and immune-molecular aspects.* Melanoma Manag, 2020. **7**(2): p. MMT44.
4. Nguyen, K., E. Hignett, and A. Khachemoune, *Current and emerging treatment options for metastatic melanoma: a focused review.* Dermatol Online J, 2020. **26**(7).
5. Li, Y.F., et al., *A Review of MicroRNA in Uveal Melanoma.* Onco Targets Ther, 2020. **13**: p. 6351-6359.
6. Dimitriou, F., et al., *The World of Melanoma: Epidemiologic, Genetic, and Anatomic Differences of Melanoma Across the Globe.* Curr Oncol Rep, 2018. **20**(11): p. 87.

7. Zikich, D., J. Schachter, and M.J. Besser, *Immunotherapy for the management of advanced melanoma: the next steps.* Am J Clin Dermatol, 2013. **14**(4): p. 261-72.
8. Leonardi, G.C., et al., *Cutaneous melanoma: From pathogenesis to therapy (Review).* Int J Oncol, 2018. **52**(4): p. 1071-1080.
9. Amaravadi, R.K., A.C. Kimmelman, and J. Debnath, *Targeting Autophagy in Cancer: Recent Advances and Future Directions.* Cancer Discov, 2019. **9**(9): p. 1167-1181.
10. Gil, J., et al., *The BAX gene as a candidate for negative autophagy-related genes regulator on mRNA levels in colorectal cancer.* Med Oncol, 2017. **34**(2): p. 16.
11. Lin, Q.G., et al., *Development of prognostic index based on autophagy-related genes analysis in breast cancer.* Aging (Albany NY), 2020. **12**(2): p. 1366-1376.
12. Luo, M.S., G.J. Huang, and H.B. Liu, *An autophagy-related model of 4 key genes for predicting prognosis of patients with laryngeal cancer.* Medicine (Baltimore), 2020. **99**(30): p. e21163.
13. Niu, Y., et al., *A Novel Scoring System for Pivotal Autophagy-Related Genes Predicts Outcomes after Chemotherapy in Advanced Ovarian Cancer Patients.* Cancer Epidemiol Biomarkers Prev, 2019. **28**(12): p. 2106-2114.
14. Jiang, G.M., et al., *The relationship between autophagy and the immune system and its applications for tumor immunotherapy.* Mol Cancer, 2019. **18**(1): p. 17.
15. Huang, Z., et al., *Genome-Wide Identification of a Novel Autophagy-Related Signature for Colorectal Cancer.* Dose Response, 2019. **17**(4): p. 1559325819894179.
16. Kazimierczak, U., et al., *BNIP3L Is a New Autophagy Related Prognostic Biomarker for Melanoma Patients Treated With AGI-101H.* Anticancer Res, 2020. **40**(7): p. 3723-3732.
17. Kim, J.Y., et al., *Autophagy induction can regulate skin pigmentation by causing melanosome degradation in keratinocytes and melanocytes.* Pigment Cell Melanoma Res, 2020. **33**(3): p. 403-415.
18. Zhang, X., et al., *CX-F9, a novel RSK2 inhibitor, suppresses cutaneous melanoma cells proliferation and metastasis through regulating autophagy.* Biochem Pharmacol, 2019. **168**: p. 14-25.
19. Yu, T., J. Zuber, and J. Li, *Targeting autophagy in skin diseases.* J Mol Med (Berl), 2015. **93**(1): p. 31-8.
20. Liu, H., et al., *Down-regulation of autophagy-related protein 5 (ATG5) contributes to the pathogenesis of early-stage cutaneous melanoma.* Sci Transl Med, 2013. **5**(202): p. 202ra123.
21. Wan, Q., et al., *Development and validation of autophagy-related-gene biomarker and nomogram for predicting the survival of cutaneous melanoma.* IUBMB Life, 2020. **72**(7): p. 1364-1378.
22. Amin, M.B., et al., *The Eighth Edition AJCC Cancer Staging Manual: Continuing to build a bridge from a population-based to a more "personalized" approach to cancer staging.* CA Cancer J Clin, 2017. **67**(2): p. 93-99.
23. Deng, J., et al., *Comparison of the staging of regional lymph nodes using the sixth and seventh editions of the tumor-node-metastasis (TNM) classification system for the evaluation of overall*

survival in gastric cancer patients: findings of a case-control analysis involving a single institution in China. Surgery, 2014. **156**(1): p. 64-74.

24. Jehn, C.F., et al., *Influence of comorbidity, age and performance status on treatment efficacy and safety of cetuximab plus irinotecan in irinotecan-refractory elderly patients with metastatic colorectal cancer.* Eur J Cancer, 2014. **50**(7): p. 1269-75.
25. Wang, C.B., et al., *Impact of Tumor Location and Variables Associated With Overall Survival in Patients With Colorectal Cancer: A Mayo Clinic Colon and Rectal Cancer Registry Study.* Front Oncol, 2019. **9**: p. 76.
26. Balachandran, V.P., et al., *Nomograms in oncology: more than meets the eye.* Lancet Oncol, 2015. **16**(4): p. e173-80.
27. Zhao, C., et al., *A gene expression signature-based nomogram model in prediction of breast cancer bone metastases.* Cancer Med, 2019. **8**(1): p. 200-208.
28. Li, T., et al., *TIMER: A Web Server for Comprehensive Analysis of Tumor-Infiltrating Immune Cells.* Cancer Res, 2017. **77**(21): p. e108-e110.
29. Tang, Z., et al., *GEPIA2: an enhanced web server for large-scale expression profiling and interactive analysis.* Nucleic Acids Res, 2019. **47**(W1): p. W556-W560.
30. Xu, X.L., et al., *Overexpression of PTK6 predicts poor prognosis in bladder cancer patients.* J Cancer, 2017. **8**(17): p. 3464-3473.
31. Peng, M., et al., *PTK6/BRK is expressed in the normal mammary gland and activated at the plasma membrane in breast tumors.* Oncotarget, 2014. **5**(15): p. 6038-48.
32. Ito, K., et al., *PTK6 Inhibition Suppresses Metastases of Triple-Negative Breast Cancer via SNAIL-Dependent E-Cadherin Regulation.* Cancer Res, 2016. **76**(15): p. 4406-17.
33. Xiao, C., et al., *Inhibition of CaMKII-mediated c-FLIP expression sensitizes malignant melanoma cells to TRAIL-induced apoptosis.* Exp Cell Res, 2005. **304**(1): p. 244-55.
34. Safa, A.R., et al., *c-FLIP, a Novel Biomarker for Cancer Prognosis, Immunosuppression, Alzheimer's Disease, Chronic Obstructive Pulmonary Disease (COPD), and a Rationale Therapeutic Target.* Biomark J, 2019. **5**(1).
35. Tian, F., et al., *Expression of c-FLIP in malignant melanoma, and its relationship with the clinicopathological features of the disease.* Clin Exp Dermatol, 2012. **37**(3): p. 259-65.
36. Shao, Y., et al., *NF-kappaB Regulation of c-FLIP Promotes TNFalpha-Mediated RAF Inhibitor Resistance in Melanoma.* J Invest Dermatol, 2015. **135**(7): p. 1839-1848.
37. Lee, H.J., et al., *DNAJB9 Inhibits p53-Dependent Oncogene-Induced Senescence and Induces Cell Transformation.* Mol Cells, 2020. **43**(4): p. 397-407.
38. Shin, W.S., et al., *PTK6 Localized at the Plasma Membrane Promotes Cell Proliferation and MigratiOn Through Phosphorylation of Eps8.* J Cell Biochem, 2017. **118**(9): p. 2887-2895.

Supplementary

Supplementary Figure s5 is not available with this version.

Figures

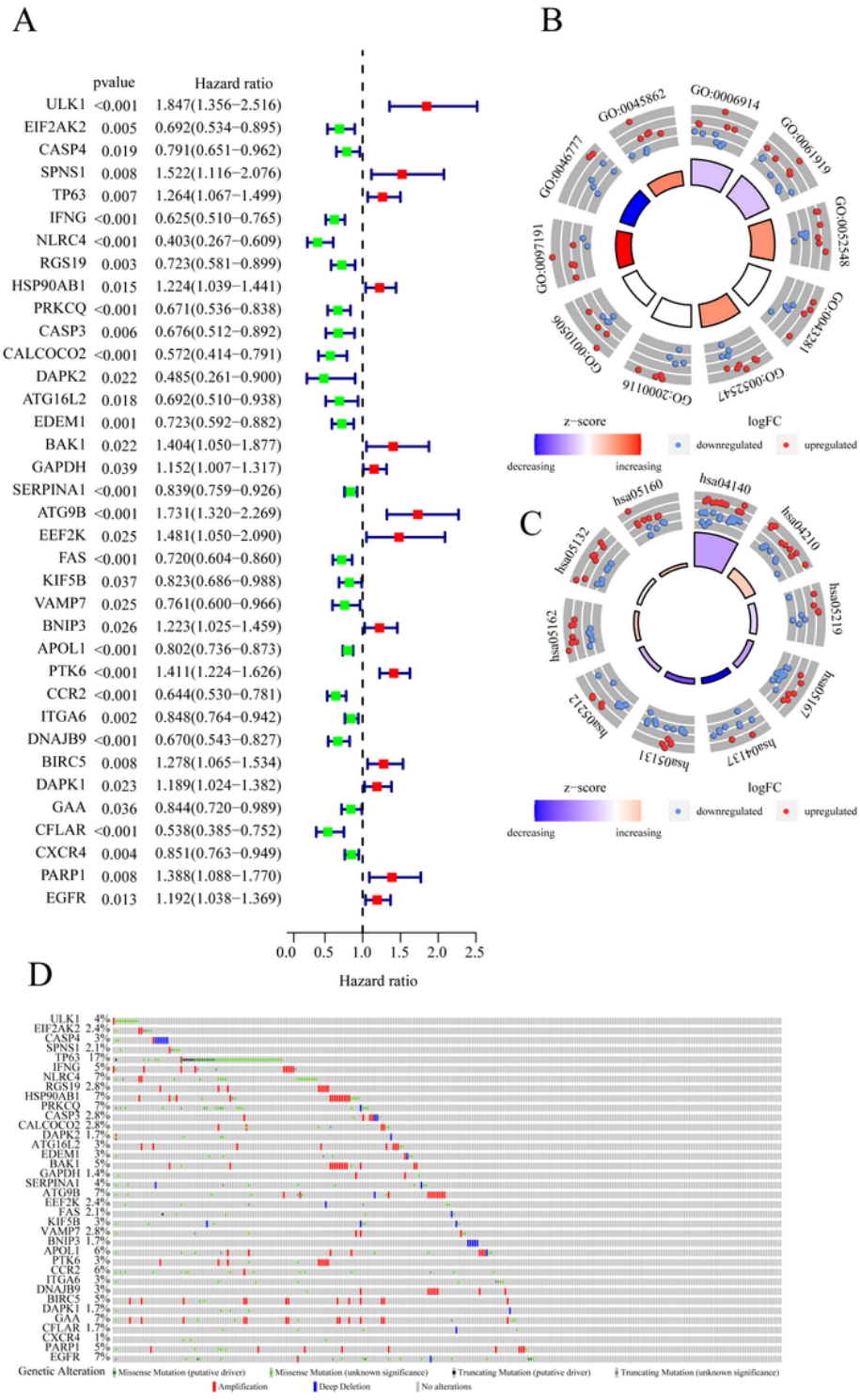

Figure 1

Expression profile and prognostic value of ARGs. (A) Risk ratio forest plot showed the prognostic value of the genes, (B) GO analysis revealed the biological processed and molecular functions involved in 36 prognostic-related ARGs, (C) KEGG shows the signaling pathways involved in 36 prognostic-related ARGs, (D) Mutations in prognosis-related ARGs. A total of 13 genes have a mutation rate ≥ 5%, of which TP63 is the most frequently mutated gene (17%).

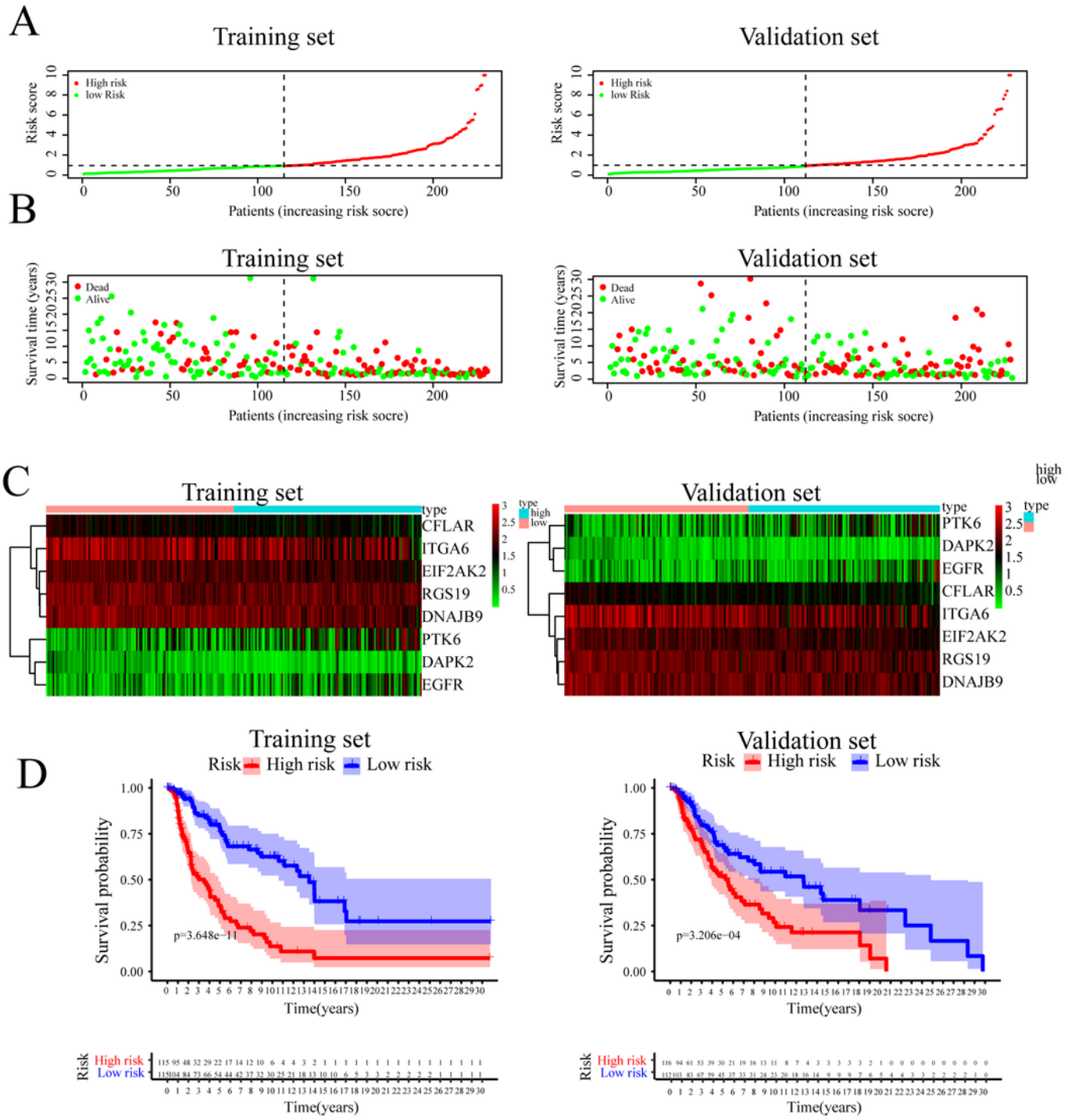

Figure 2

Development of a prognostic index based on ARGs. (A) Distribution of prognostic index, (B) Survival status of patients in different groups, (C) Heat map of the expression profile of 8-autophagy-related genes, (D) Kaplan-Meier survival curves of 8-autophagy-related genes.

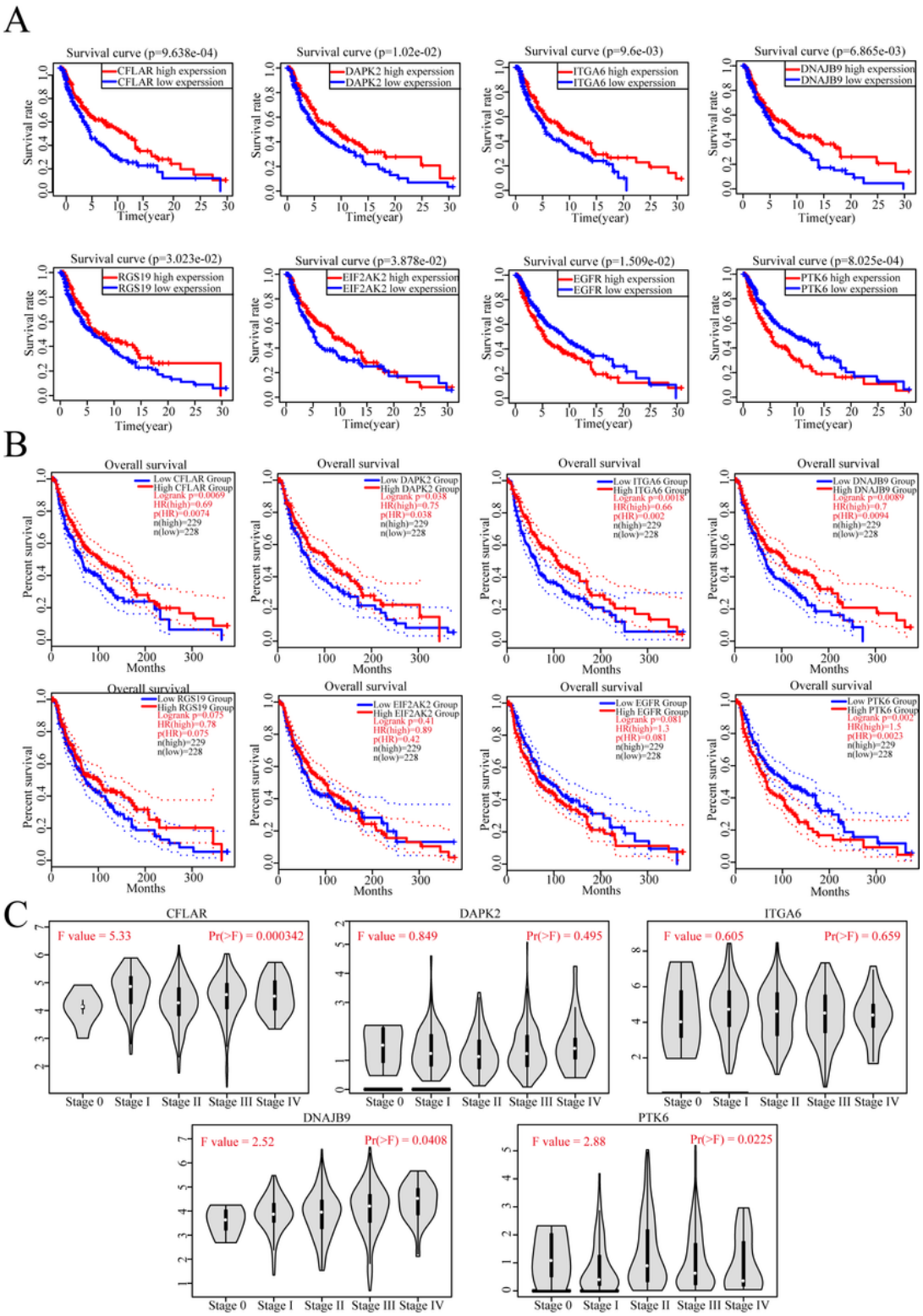

Figure 3

Validation of significant autophagy-related genes index (A) Survival curve of 8-ARGs based on TCGA and GETx database, (B) Overall survival of 8-ARGs based on GEPIA tools. Cutoff-High(%): Samples with

expression level higher than this threshold are considered as the high-expression cohort. Cutoff-Low(%): Samples with expression level lower than this threshold are considered the low-expression cohort., (C) This feature generates expression violin plots of significant ARGs based on patient pathological stage. The method for differential gene expression analysis is one-way ANOVA, using pathological stage as variable for calculating differential expression.

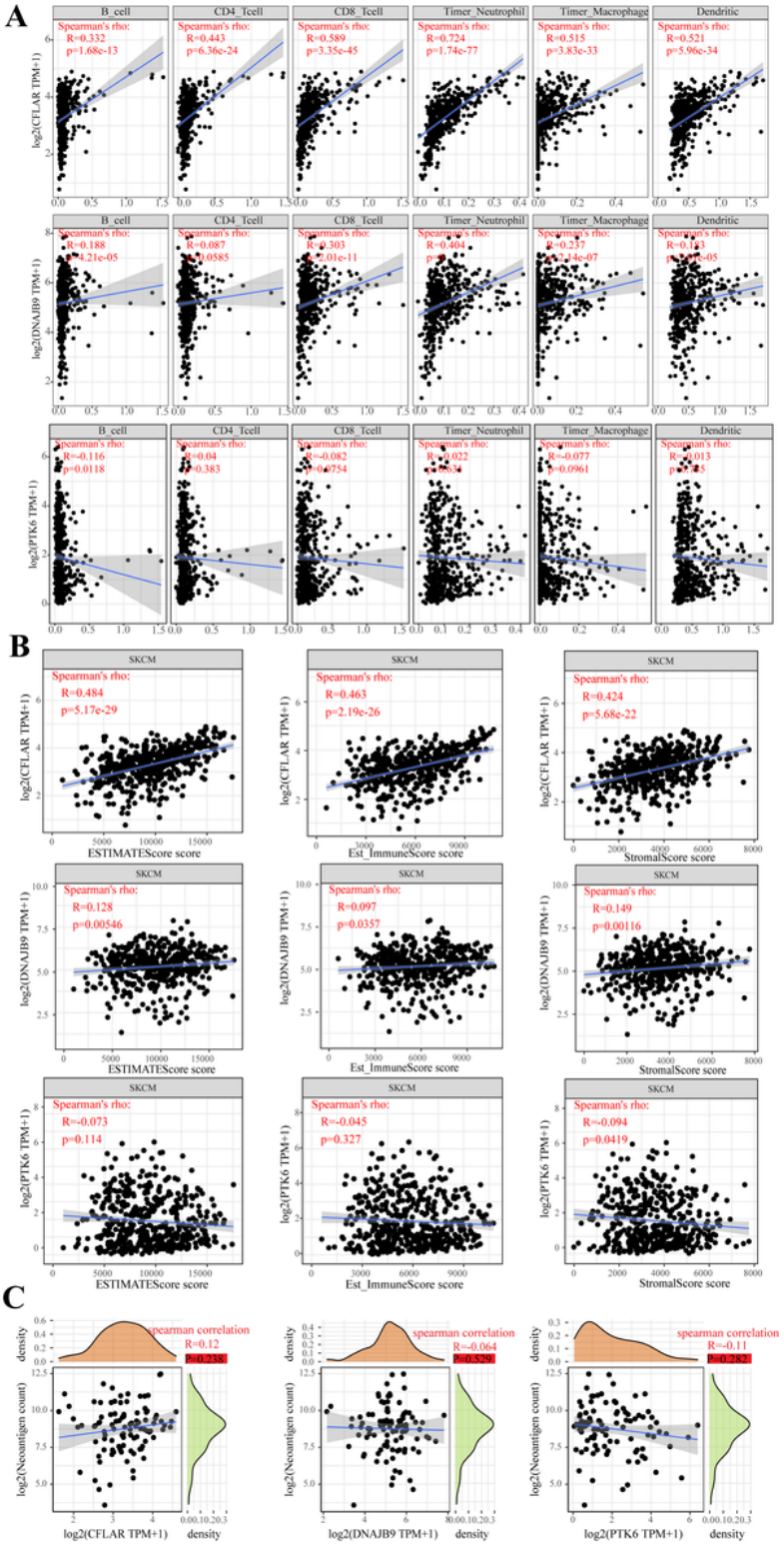

Figure 4

Relationship between high risk ARGs, low risk ARGs and immunity in SKCM (A) Correlation of significant ARGs with immune infiltration level. Survival curve of 8-autophagy-related genes. Six immune infiltrating scores was downloaded from TIMER database, (B) Relationship of significant ARGs with ImmuneScore and StromalScrore, (C) Relationship of significant ARGs with neoantigen.

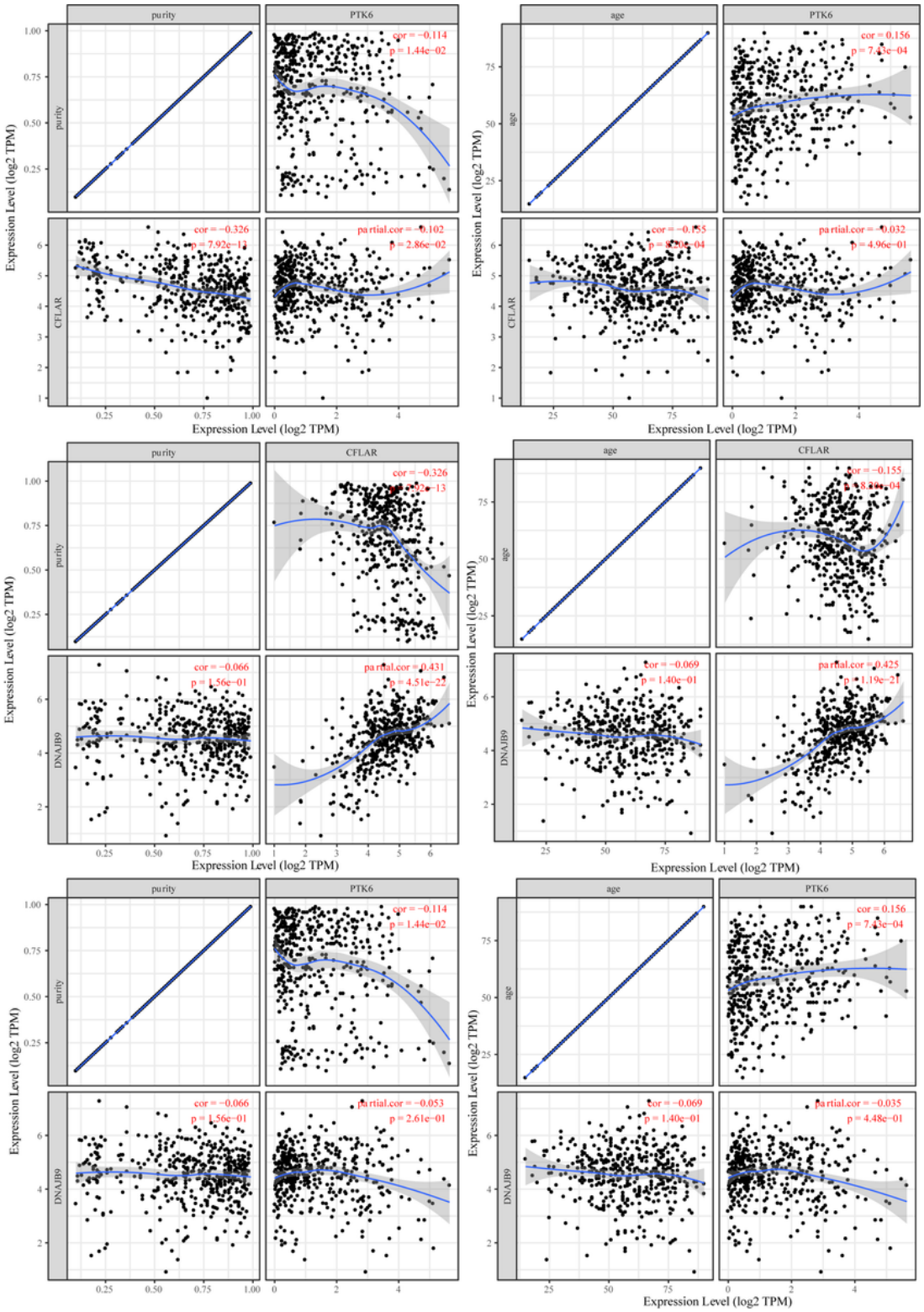

Figure 5

Correlation between high risk ARGs and low risk ARGs in patients with SKCM TIMER online tool was applied to study the correlation of high risk ARGs and low risk ARGs in SKCM adjusted by tumor purity or age.

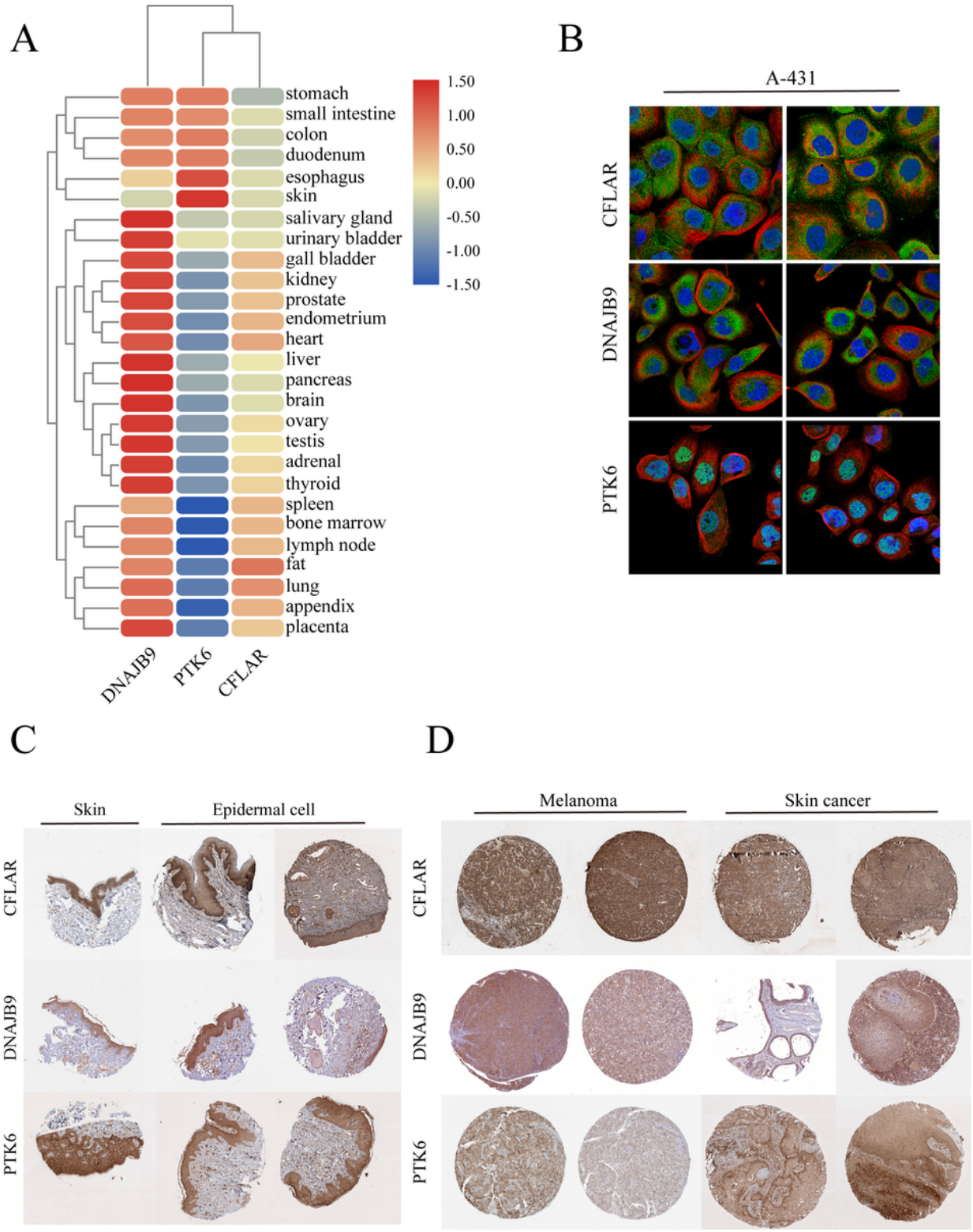

Figure 6

Tissue profile and cell localization of CFLAR, DNAJB9 and PTK6 (A) HPA mRNA expression tissue profile, (B) Cell localization of CFLAR, DNAJB9 and PTK6 in A-431 cell lines. Green indicates antibody, blue

indicates nucleus, red indicates microtubules, (C) Staining of CFLAR, DNAJB9 and PTK6 in skin tissue, (D) protein expression level of CFLAR, DNAJB9 and PTK6 in melanoma and skin cancer.

Supplementary Files

This is a list of supplementary files associated with this preprint. Click to download.

- FigureS1.tif
- FigureS2.tif
- FigureS3.tif
- FigureS4.tif
- GraphicalAbstract.tif